

FULL-LENGTH REPORT

# Slow-delta phase concentration marks improved temporal expectations based on the passage of time

ANNA WILSCH,<sup>a</sup> MOLLY J. HENRY,<sup>a</sup> BJÖRN HERRMANN,<sup>a</sup> BURKHARD MAESS,<sup>b</sup> AND JONAS OBLESER<sup>a,c</sup>

<sup>a</sup>Max Planck Research Group “Auditory Cognition”, Max Planck Institute for Human Cognitive and Brain Sciences, Leipzig, Germany

<sup>b</sup>MEG and Cortical Networks, Max Planck Institute for Human Cognitive and Brain Sciences, Leipzig, Germany

<sup>c</sup>Department of Psychology, University of Lübeck, Lübeck, Germany

## Abstract

Temporal expectations enhance neural encoding precision, reflected in optimized alignment of slow neural oscillatory phase, and facilitate subsequent stimulus processing. If an event’s exact occurrence time is unknown, temporal expectations arise solely from the passage of time. Here, we show that this specific type of temporal expectation is also reflected in neural phase organization. While undergoing magnetoencephalography, participants performed an auditory-delayed matching-to-sample task with two syllables (S1, S2). Critically, S1-onset time varied in the 0.6–1.8-s (i.e., 0.6–1.7 Hz) range. Increasing S1-onset times led to increased slow-delta (0.6–0.9 Hz) phase coherence over right frontotemporal sensors during S1 encoding. Moreover, individuals with higher slow-delta coherence showed decreased alpha power (8–13 Hz) during subsequent memory retention. In sum, temporal expectations based on the passage of time optimize the precise alignment of neural oscillatory phase with an expected stimulus.

**Descriptors:** Slow-delta, Phase coherence, Temporal expectations, MEG, Delayed match-to-sample

Temporal orienting guides the focus of attention to a point in time when a target stimulus is expected to occur (i.e., “temporal expectations”; Coull & Nobre, 1998). The ability to direct attention in time is testimony to the temporal flexibility of attentional functions in the human brain (Nobre, 2001) and is gaining scientific interest from both a psychological and a neuroscientific viewpoint.

A distinction can be made between different sources of temporal expectations. First, the presentation of a symbolic temporal cue may allow the prediction of the onset time of an expected event (referred to by Nobre and colleagues as “controlled” temporal expectation; Coull & Nobre, 1998). Second, temporal expectations can arise from rhythmic structure such that the onset times of each stimulus in a rhythmic sequence become highly predictable (Barnes & Jones, 2000; Jones, Moynihan, MacKenzie, & Puente, 2002; Large & Jones, 1999). Third, for a situation in which an event is certain to occur, but the exact time of occurrence is not known, temporal expectation follows a “hazard rate function,” meaning that expectation for the event’s onset increases with passage of time (referred to as “automatic” temporal expectations by Nobre, Correa, & Coull, 2007; Janssen & Shadlen, 2005). All three types of temporal expectations have been shown to enhance perceptual processing of the

expected stimulus (Correa & Nobre, 2008), which is reflected by decreasing response times (Correa, Lupiáñez, & Tudela, 2006; Doherty, Rao, Mesulam, & Nobre, 2005; Nobre, 2001; Rohenkohl, Coull, & Nobre, 2011; Sanabria & Correa, 2013; Stefanics et al., 2010) and increasing encoding precision (Cravo, Rohenkohl, Wyart, & Nobre, 2013; Rohenkohl, Cravo, Wyart, & Nobre, 2012).

Slow neural oscillations constitute a parsimonious neural mechanism for facilitatory effects of temporal expectations (Henry & Herrmann, 2014). By this account, the brain capitalizes on temporal regularities to be in its optimal (i.e., high-excitability) state when the relevant stimulus occurs (Schroeder & Lakatos, 2009). Accordingly, expectations generated by symbolic cues about time of occurrence have been shown to reorganize slow neural oscillatory phase (Stefanics et al., 2010). For the most part, however, the relationship between the phase of slow neural oscillations and temporal expectations has been studied using rhythmically presented stimuli. In this case, neural oscillations are entrained by temporal regularities leading to increased neural phase concentration across trials in the frequency range corresponding to the stimulation rate (2.5 Hz: Cravo et al., 2013; 1.5 Hz: Lakatos, Karmos, Mehta, Ulbert, & Schroeder, 2008; 3.95 Hz: Herrmann, Henry, Grigutsch, & Obleser, 2013; 3 Hz: Henry & Obleser, 2012; 0.67 Hz: Lakatos, Schroeder, Leitman, & Javitt, 2013). However, to date it is unknown whether instantaneous temporal expectations resulting from passage of time (i.e., as a function of foreperiod duration) are related to the organization of delta phase in a similar manner. If so, we expect delta phase coherence to increase with increasing temporal expectations coupled to the passage of time.

This research was funded by the Max Planck Society. AW, MJH, BH, and JO are funded by a Max Planck Research Group grant awarded to JO. The authors are grateful to Yvonne Wolf who helped record all MEG data.

Address correspondence to: Anna Wilsch or Jonas Obleser, Max Planck Institute for Human Cognitive and Brain Sciences, Stephanstrasse 1a, 04103 Leipzig, Germany. E-mail: wilsch@cbs.mpg.de or obleser@cbs.mpg.de

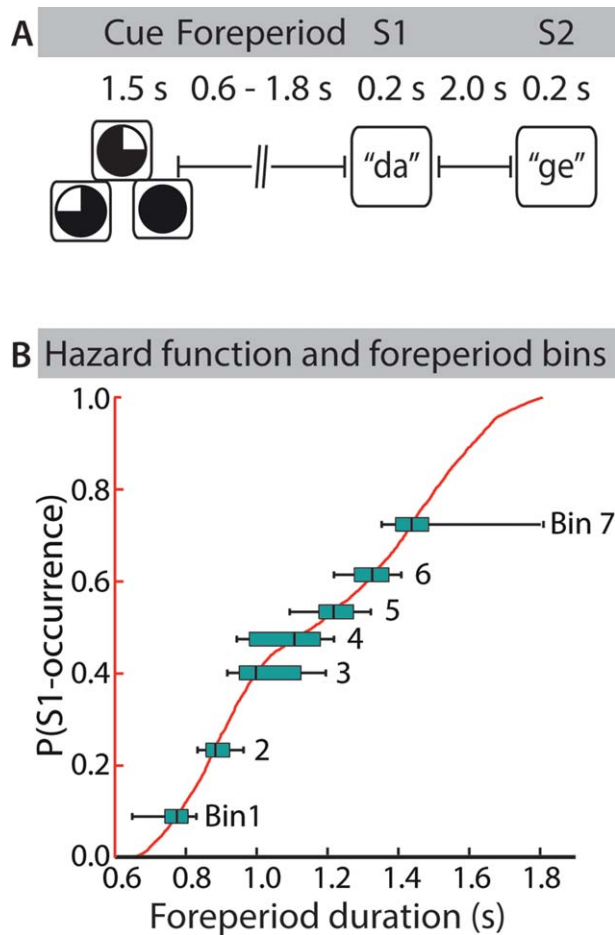


**Figure 1.** Experimental manipulation and characteristics of the foreperiod. **A:** Outline of a trial. Each trial started with the presentation of one of three visual cues. The foreperiod between cue offset and S1 onset varied between 0.6 and 1.8 s. Both syllables lasted 0.2 s. The first syllable had to be retained in memory for 2 s, then the second syllable was presented. Approximately 1 s after S2 presentation, a response prompt appeared, and subjects indicated whether S2 started with the same or with a different consonant as S1. **B:** Temporal hazard function and the foreperiod bins. The hazard function was calculated as the cumulative probability of S1 occurrence according to the foreperiod duration, across the experiment. Seven foreperiod bins are depicted by means of box plots, where the black central line illustrates the median foreperiod of each bin, linearly spaced across all trials. Whiskers indicate the 25%- and 75%- percentiles of trials of each bin.

So far, temporal expectations have most successfully been studied with near-threshold stimuli (Cravo et al., 2013; Lawrance, Harper, Cooke, & Schnupp, 2014; Rohenkohl et al., 2012) where expectation effects are behaviorally and neurally strongest (e.g., Lange & Schnuerch, 2014). In the present study, we were interested in how temporal expectations play out in a more ecologically valid setting with suprathreshold spoken syllables. Extending a previous experiment on near-threshold stimuli (Wilsch, Henry, Herrmann Maess, & Obleser, 2014), we manipulated the temporal structure of trials and the expectations coupled to the trial structure: Explicit temporal cues allowed for the formation of temporal expectations, but we hypothesized that these would be less relevant for suprathreshold stimuli. More importantly, however, stimulus-onset times were variable within a 0.6-s to 1.8-s ( $\sim 1.7$  Hz to  $\sim 0.6$  Hz) range, and longer foreperiod durations were expected to prompt stronger temporal expectations. Our results demonstrate that slow-delta phase coher-

ence is a sensitive marker of the degree of temporal expectations for the occurrence of suprathreshold stimuli.

## Method

### Participants

Ten healthy right-handed participants (ranging in age from 24 to 36; five females) took part in this study. All participants had self-reported normal hearing. Participants were fully debriefed about the nature and goals of this study, and received financial compensation of 7 € per hour for their participation. The study was approved by the local ethics committee (University of Leipzig), and written informed consent was obtained from all participants prior to testing.

### Experimental Task and Stimuli

Two spoken syllables were presented per trial, and participants had to indicate whether the syllables shared the same initial consonant by responding “same” or “different.” The time course of an example trial is depicted in Figure 1A. Each trial began with the onset of a fixation cross, followed by a visual cue (fixation–cue interval jittered between 750 ms to 1,250 ms). Cues were presented for 1,500 ms and indicated the approximate onset time of the first syllable, S1. Note that the cue presentation time was comparably long but fixed. Thus, the foreperiod leading up to the first target S1 was measured from the offset time of the cue. Participants had to retain S1 in memory during a 2-s retention period before the presentation of the second syllable, S2.

Critically, the foreperiod duration varied from trial to trial between 0.6 to 1.8 s. The variable foreperiod duration induced temporal expectations by increasing the instantaneous probability of S1-onset occurrence with the passage of time (see Figure 1B). Furthermore, foreperiod durations were split into three groups according to the preceding cue: “early,” “late,” and “neutral.” That is, S1-onset times for early and late cues were randomly drawn from Gaussian distributions (early:  $\mu = 850$  ms,  $\sigma = 85$  ms; late:  $\mu = 1,300$  ms,  $\sigma = 130$  ms). S1-onset times after neutral cues were randomly drawn from a uniform distribution ranging between 700 ms and 1,500 ms. S1 and S2 stimuli consisted of four different syllables: “da,” “de,” “ga,” and “ge” spoken by a female voice. For more details on the experimental task and stimuli, see Wilsch et al. (2014).

### Procedure

While brain activity was recorded with magnetoencephalography (MEG; see below), participants performed 360 trials, organized in 18 blocks of 20 trials each. Cue type (early, late, neutral) was constant within a block, and participants were informed at the start of each block about the type of temporal cue they would receive on each trial. The order of trials within a block and order of blocks were randomized for each participant. Button assignments were counter-balanced across participants, such that half of the participants indicated that S1–S2 shared the same initial consonant using the left button, and half did so with the right button. The testing took approximately 1.5 h per participant and was conducted within one session.

### Data Recording and Analysis

Participants were seated in an electromagnetically shielded room (Vacuumschmelze, Hanau, Germany). Magnetic fields were recorded using a 306-sensor Neuromag Vectorview MEG (Elekta, Helsinki, Finland) with 204 orthogonal planar gradiometers and 102 magnetometers at 102 locations. Two electrode pairs recorded

a bipolar electrooculogram (EOG) for horizontal and vertical eye movements. The participants' head positions were monitored during the measurement by five head-position indicator (HPI) coils. Signals were sampled at a rate of 1000 Hz with a bandwidth ranging from direct current (DC) to 330 Hz. The signal space separation method was applied offline to suppress external interferences in the data and to transform individual data to a default head position that allows statistical analyses across participants in sensor space (Taulu, Kajola, & Simola, 2004). Subsequent data analyses were carried out with MATLAB (The MathWorks Inc., Natick, MA) and the FieldTrip toolbox (Oostenveld, Fries, Maris, & Schoffelen, 2011) using only trials to which correct responses were provided ("correct trials," percentage correct > 98%). Analyses were conducted using only the 204 gradiometer sensors, as they are most sensitive to magnetic fields originating directly underneath the sensor (Hämäläinen, Hari, Ilmoniemi, Knuutila, & Lounasmaa, 1993). The continuous data were filtered offline with a 70 Hz low-pass filter. No high-pass filter was applied in order to analyze neural oscillations in the slow-delta (< 1 Hz) frequency band.

Subsequently, trial epochs ranging from  $-4$  to  $7$  s time-locked to the onset of S1 were extracted, and downsampled to 200 Hz. First, epochs with strong artifacts were rejected when the signal range at any sensor exceeded 800 pT/m (gradiometer). Then, the mean of each epoch was subtracted, and independent component analysis (ICA) was applied to the epochs in order to exclude artifacts mainly due to eye blinks and heartbeat. Following ICA, remaining epochs containing artifacts exceeding a threshold of 200 pT/m were rejected.

### Time-Frequency Representations (TFRs)

Time-frequency representations (TFRs) were calculated for the pre-processed 11-s epochs for each trial (with 20-ms time resolution) and for frequencies ranging between 0.5 Hz to 20 Hz (logarithmically spaced, in 20 bins). Time-domain data were convolved with a Hann taper, with an adaptive width of two to four cycles per frequency (i.e., 2 cycles for 0.5–1.6 Hz, 3 cycles for 1.9–9.2 Hz, and 4 cycles for 11.1–20 Hz). The output of the analysis was complex Fourier data, allowing for analyses of phase and of power.

### Correlation of TFRs with S1-Onset Time

Instantaneous temporal expectations increase with longer foreperiod durations (Nobre et al., 2007). Hence, in order to test whether slow-delta phase coherence, or other measures of slow-delta oscillatory activity, reflect the strength of temporal expectations, measures of slow neural oscillatory activity were correlated with foreperiod duration. To this end, trials were grouped into seven bins according to their individual foreperiod duration according to the following procedure: First, all trials for each participant were sorted in order of increasing foreperiod duration. Then, seven trials were selected that were equally (linearly) spaced in terms of foreperiod duration (in seconds) and that also spanned the entire set of durations. These trials served as bin centers. A bin contained 37 adjacent trials with shorter foreperiod durations and 37 adjacent trials with longer foreperiod durations. That way, the bin centers were equal to the median of each bin, which served as a regressor in the subsequent correlation analyses. This procedure ensures equal trial numbers per bin, whereas bins have variable widths in terms of foreperiod duration. See Figure 1B for an example.

Next, three neural activity measures were calculated for each time-frequency sensor bin and for each foreperiod bin: Intertrial phase coherence (ITPC; Lachaux, Rodriguez, Martinerie, & Var-

ela, 1999), total power, and evoked power (David, Kilner, & Friston, 2006; Ding & Simon, 2013). ITPC corresponds to the magnitude of the amplitude-normalized complex numbers averaged across trials of the TFR estimates for each time-frequency bin, channel, and foreperiod bin (Thorne, De Vos, Viola, & Debener, 2011). Total power was expressed as the average power (squared magnitude of the complex-valued TFR estimates) across single trials (see below), while evoked power was calculated for each channel and foreperiod bin by first averaging single-trial time domain data, then calculating the power as the squared magnitude of the complex-valued TFR estimation.

Lastly, we normalized total power and evoked power by means of  $z$  transform, taking the full 11-s epoch as reference. Note that our experimental design did not allow the definition of a long enough time interval to serve as a conventional reference baseline for subtraction. For the  $z$  transform, we computed the trial mean and the trial standard deviation ( $SD$ ) of power in each trial, channel, and frequency bin.  $Z$ -transformed total power as a function of time (i.e., for each individual time bin) was then computed by first subtracting the trial mean and subsequently dividing by the trial  $SD$ . Finally, normalized power was averaged across trials within each foreperiod bin at each time-frequency bin and channel. Evoked power normalization was performed on overall power representations per foreperiod bin at each time-frequency-channel bin, again by subtracting the mean over time bins and dividing by the  $SD$  across time bins.

Prior to the statistical analyses (see next section), gradiometer pairs were combined by means of averaging across two gradiometers of a pair for ITPC, total power, and evoked power, respectively. For each dependent measure, this procedure resulted in one value for each time point, frequency bin, sensor position, and foreperiod duration bin.

### Statistical Analysis

Behavioral dependent measures (i.e., proportion correct and response times) were correlated with foreperiod duration in order to test for increases in performance with increasing temporal expectations due to longer foreperiods. Additionally, behavioral measures were analyzed with separate one-way repeated measures analyses of variance (ANOVAs; early, late, and neutral) to test for effects of temporal cues.

Statistical analyses of the correlation of foreperiod duration with ITPC, total power, and evoked power followed a multilevel approach (Obleser, Wöstmann, Hellbernd, Wilsch, & Maess, 2012; van Dijk, Nieuwenhuis, & Jensen, 2010; Wilsch et al., 2014): On the first (single-subject) level, the median duration of the seven foreperiod bins was correlated with a particular dependent measure in each time-frequency-channel bin. Statistical tests were performed within the framework of Fieldtrip's independent samples regression  $t$  test with contrast coefficients corresponding to the medians of the foreperiod duration bins. Linear coefficients for all contrasts (ITPC, total power, evoked power) were obtained for each time-frequency bin at each of the 102 sensor positions.

The focus of the correlation analysis was on effects in the frequency range that corresponded to the range of rates that were most likely to correspond to temporal expectations due to foreperiod duration. Here, foreperiod durations varied from 0.6 s to 1.8 s, and we hypothesized that temporal orienting within this range of durations would be reflected in phase organization in the corresponding  $\sim 0.6$  to  $\sim 1.7$  Hz frequency range. Therefore, the statistical analyses on the second (group) level were conducted on exactly that frequency range (i.e., 0.6–1.7 Hz). Our time window of interest

was  $-0.5$  to  $0.5$  s time-locked to S1 onset in order to cover pre- and peristimulus effects after cue presentation.

In a previous study, we observed variations in alpha power during the S1 retention period due to cued temporal expectations (Wilsch et al., 2014). Thus, in the current study we additionally examined the correlation between alpha power (8–13 Hz) and foreperiod duration using the same multilevel correlation analysis described above. In order to capture activity during retention, the time window of interest ranged from  $-0.5$  to  $2.5$  s time-locked to S1.

For all correlation analyses, linear coefficients resulting from the single-subject first-level statistics were tested on the group level against zero with cluster-based permutation tests (dependent samples  $t$  tests, 1,000 iterations; Maris and Oostenveld, 2007). The cluster approach protects against inflated Type 1 error due to multiple comparisons. All cluster tests were one tailed in favor of a positive correlation for the delta frequency band and one tailed in favor of a negative correlation for the alpha frequency band and were thus considered significant when  $p < .05$ .

Post hoc correlations were conducted on the clusters resulting from the correlations between delta ITPC and alpha power with foreperiod duration (see below). Here, delta ITPC and alpha power were averaged across the channel–time–frequency bins belonging to their respective significant cluster. Averages were calculated separately for each foreperiod bin and for each subject. Then two correlations were calculated, one across foreperiod bins and one across participants. For the correlation across foreperiod bins, the delta ITPC values and the alpha power values were averaged across participants, resulting in a single delta ITPC and a single alpha power value per foreperiod bin, which were then correlated. Similarly, for the correlation across participants, dependent measures were averaged over foreperiod durations, yielding a single delta ITPC and a single alpha power value per participant, which were then correlated.

Effect sizes for all measures reported were calculated by estimating the effect size measure  $r_{\text{equivalent}}$  (denoted  $r$ ), which is bound between 0 and 1 (Rosenthal, 1994). In the case of cluster tests where  $t$  statistics were obtained for all time–frequency–channel bins,  $r$  values were averaged across all bins belonging to a significant cluster (denoted  $R$ ).

## Results

Behavioral performance did not vary with foreperiod duration (accuracy:  $t(9) = -0.017$ ,  $p = .507$ ,  $r = .006$ ; response times:  $t(9) = 0.89$ ,  $p = .19$ ,  $r = .28$ ) or cueing condition (accuracy:  $F(2,18) = 0.35$ ,  $p = .71$ ,  $r = .18$ , response times:  $F(2,18) = 0.10$ ,  $p = .91$ ,  $r = .02$ ), most likely because performance was at ceiling for all conditions ( $>98\%$  accuracy). In order to test whether explicit temporal cues elicited variations in neural measures reflecting temporal expectations, ITPC, total power, and evoked power were compared across the three cueing conditions (early, late, neutral) using multilevel cluster  $t$  tests. These statistical contrasts on ITPC, total power, and evoked power did not reveal any effects beyond cue evoked responses (data not shown here). Therefore, we will focus on the effects of temporal expectations induced by the passage of time as indexed by correlations between brain measures (ITPC, total power, evoked power) and foreperiod duration.

With respect to delta ITPC, statistical analyses revealed one positive cluster ( $-0.5$  to  $0.46$  s,  $p = .045$ ,  $R = .63$ ) at right fronto-temporal sensors (see Figure 2A,D) ranging from  $0.6$  to  $0.9$  Hz. This effect peaked between  $0.7$  and  $0.9$  Hz and at  $120$  ms, that is, around S1 onset. Figure 2B illustrates the enhancement in slow-delta ITPC and phase distributions for the first and last foreperiod

bins. ITPC is consistent with auditory generators (Figure 2B, left and right topographical plots; Herrmann et al., 2013). As illustrated for two single participants, the phase concentration (as indexed by the length of the resultant vector) was higher in the last bin compared to the first (Figure 2D).

Unsurprisingly, analyses on evoked power revealed qualitatively similar effects as for ITPC (e.g., Henry & Obleser, 2012). Here, however, the slow-delta cluster did not attain significance on a conventional 5% level (positive cluster:  $-0.5$  to  $0.5$  s,  $p = .12$ ,  $R = .64$ ). Note that the strong similarity between ITPC and evoked power, as well as their difference in the statistical effect will be addressed more thoroughly in the Discussion section. Similarly, total power did not present any clusters in the slow-delta range (see Figure 2, center and right panel).

The analysis on alpha power revealed a centrally distributed negative cluster ( $1.12$ – $1.92$  s,  $p = .013$ ,  $R = .71$ ) indicating less alpha power during S1 retention after longer foreperiods (see Figure 3A). This alpha power decrease and the delta ITPC increase both reflect the brain's sensitivity to variable foreperiods, raising the question whether delta ITPC and alpha power are mutually dependent. Therefore, we correlated delta ITPC and alpha power (data were averaged across participants) across foreperiod durations, which revealed a negative dependency ( $r = -.77$ ,  $p = .044$ ,  $df = 5$ ; see Figure 3B, left). For each participant individually, this ITPC–alpha power correlation was calculated and subsequently transformed to Fisher's  $z$ . Mean Fisher's  $z$  coefficients were significantly smaller than zero,  $t(6) = -3.10$ ,  $p = .013$ ,  $r = -.72$ . Although the partial correlation between delta ITPC and alpha power (regressing out the bins' foreperiod duration) was nonsignificant ( $r = .62$ ,  $p = .191$ ,  $df = 5$ ), this finding illustrates the modulatory effect that foreperiod duration exerts on delta phase concentration and later alpha power modulation. However, another correlation between slow-delta ITPC and alpha power across participants (data were averaged across foreperiod bins) also addressed the question of a mutual dependency of delta ITPC and alpha power and revealed another significant negative correlation ( $r = -.71$ ,  $p = .02$ ,  $df = 8$ ; see Figure 3B, right panel). Thus, participants presenting high slow-delta ITPC at S1 showed a decrease in alpha power during S1 retention, independent of foreperiod duration.

Negative effects of foreperiod duration on ITPC, total power, and evoked power were also observable (Figure 2 A–C). These effects are likely a more trivial reflection of the cue offset response shifting and being closer to S1 (i.e., in the  $-0.8$ – $0.0$ -s range relative to S1) for shorter foreperiods: The occipitoparietal distribution of these effects (see topography inlay in Figure 2A) as well as a similarly distributed effect in total power (not shown, but critically absent for the positive ITPC effect, see Figure 2A vs. 2C) imply that this negative ITPC effect was primarily caused by the change in visual stimulation at cue offset.

## Discussion

In the current study, we have shown that temporal expectations for stimulus occurrence based on the passage of time are reflected in a gradual increase of phase coherence of slow-frequency oscillatory activity. Furthermore, these temporal expectations exert also a “remote” impact and reduce the magnitude of the typical alpha power increase observed during later retention of sensory information in memory. In notable contrast to the same task using near-threshold stimuli (speech in noise; Wilsch et al., 2014), explicit temporal cues here had no discernible impact, as cues failed to elicit neural or behavioral markers of temporal expectation.

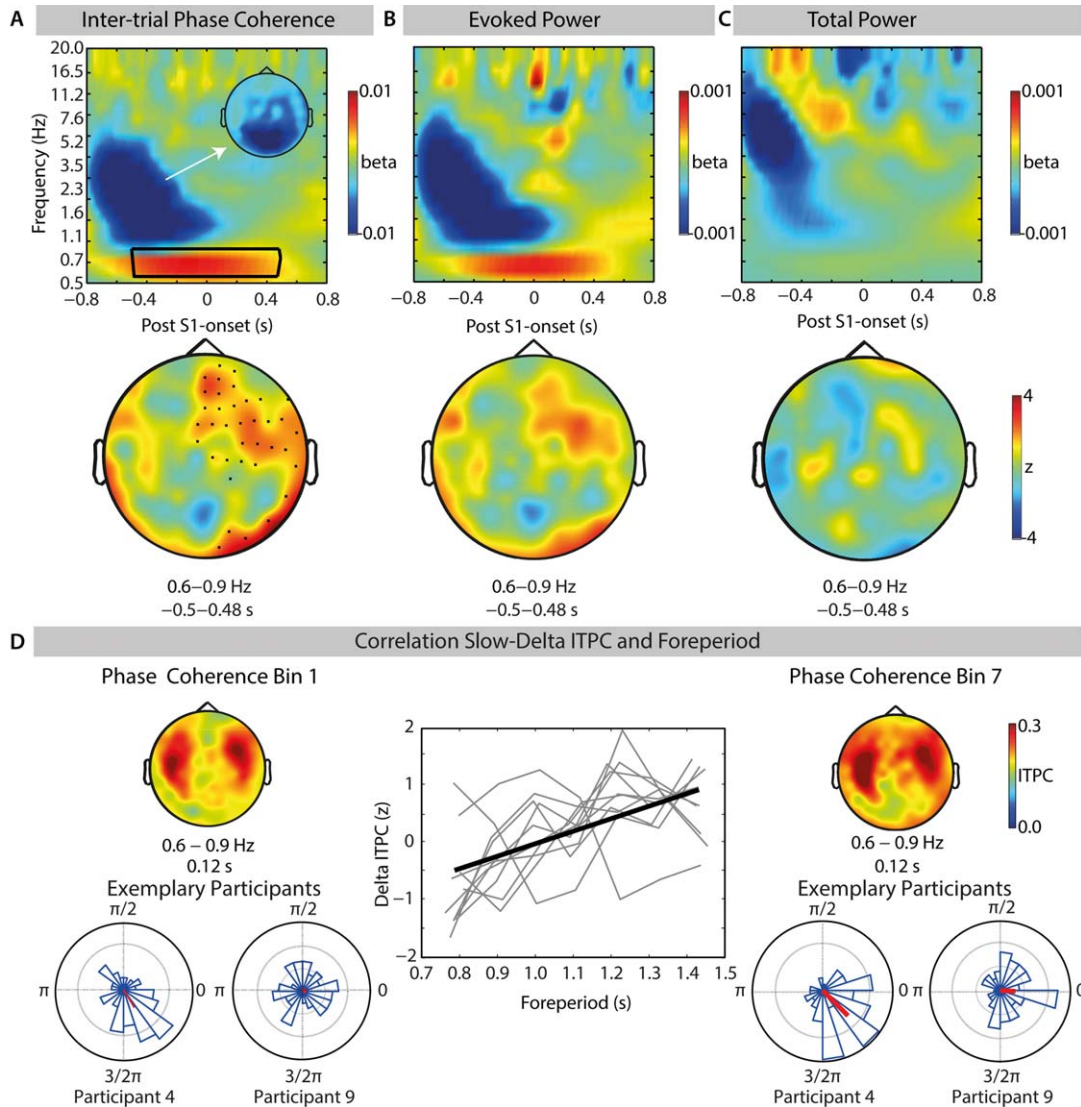


**Figure 2.** A–C: Correlation of foreperiod duration with ITPC, total power, and evoked power. A (intertrial phase coherence, ITPC), B (evoked power), and C (total power) time-frequency plots display first-level correlation coefficients (beta values averaged over participants) of the correlation between foreperiod duration (1 to 7 bins) and the respective neural measure from 0.5 to 20 Hz and  $-0.8$  to  $0.8$  s time-locked to S1 onset. Topographies illustrate the distribution of second-level  $z$  values averaged across the slow-delta range (0.6 to 0.9) during the duration of the delta effect ( $-0.5$  to  $0.48$  s). Marked channels in the left plot show the location of the significant cluster. Small topography in ITPC single plot illustrates beta values in higher frequencies averaged across all channels. **D:** Correlation of slow-delta ITPC and foreperiod duration. The central plot illustrates variations of slow-delta ITPC with foreperiod duration for each subject averaged across the significant positive cluster. The thick black line represents the average of all single-subject linear fits. Topographic plots on the left and right show slow-delta (0.6–0.9 Hz) at 0.12 s after S1 onset (peak of effect). The left plot represents ITPC in the first foreperiod bin and the right plot in last (7th) foreperiod bin. Rose plots underneath illustrate slow-delta phase distribution at 0.12 s in bin 1 (left) and bin 7 (right) of two representative participants. The red line corresponds to the resultant vector.

### Effects of Temporal Expectations on Slow-Delta Phase Concentration

For suprathreshold stimulation with highly familiar syllables, no behavioral effect of temporal expectancy occurred ( $>98\%$  accuracy). On a neural level, however, temporal expectancy affected the processing of these syllables: Very slow neural oscillations ( $<1$  Hz; corresponding to the frequency range of the so-called slow 1 band, 0.5–2 Hz; Penttonen, 2003) turned out to be a sensitive marker for variations in the strength of temporal expectation induced by varying foreperiod durations. Foreperiod duration correlated significantly with slow-delta phase coherence around the onset of the target syllable at right frontotemporal sensors. These

data fit previous observations that delta band phase locking increases with increasing probability of stimulus occurrence (Stefanics et al., 2010), but extend these to a more implicit and variable scenario of expectations formed only from the passage of time. In general, low-frequency neural oscillations have been related to neural excitability fluctuations (Lakatos et al., 2005; Steriade, Nunez, & Amzica, 1993). Our data suggest that temporal expectations as a function of foreperiod duration-tuned slow-delta oscillations to be in a high-excitable phase just before and during occurrence of the first target syllable ( $-0.5$ – $0.48$  s; covering approximately a half cycle of these very slow oscillations).

We tested for phase coherence effects specifically in the slow-delta range (0.6–1.7 Hz) because we hypothesized a correspondence

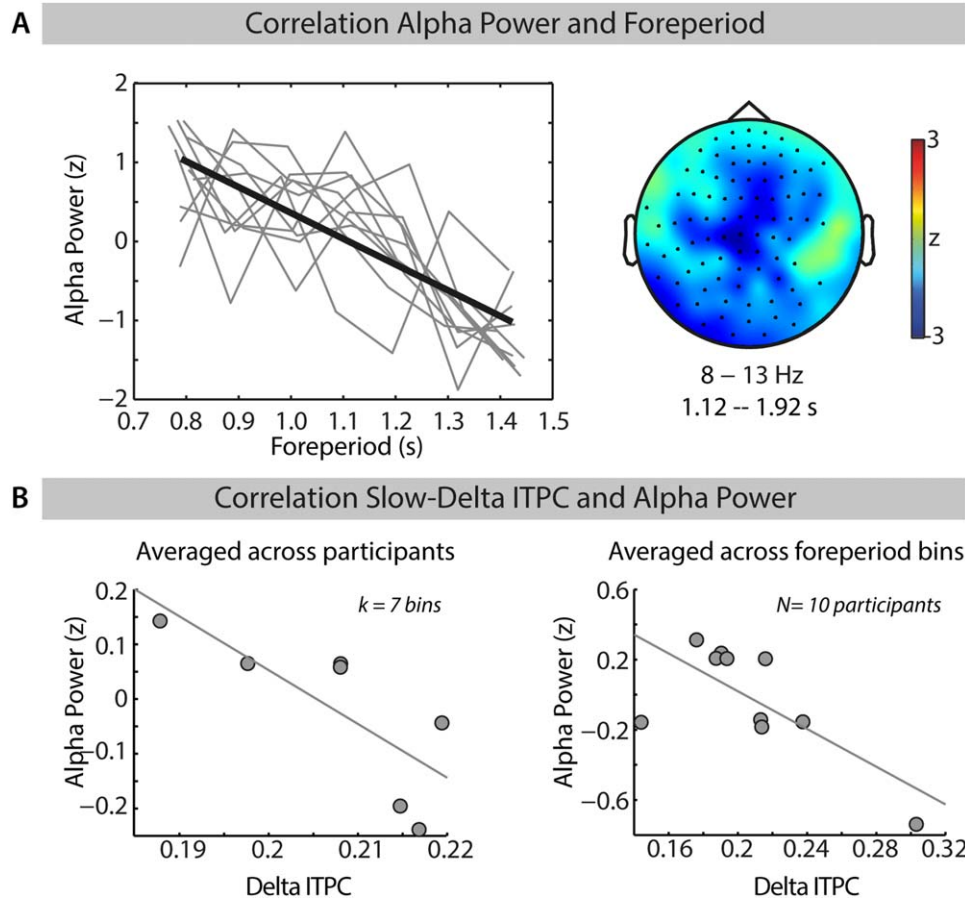


**Figure 3. A:** Correlation of foreperiod duration with alpha power. Left panel illustrates variations in alpha power with foreperiod duration for each individual subject averaged across the significant negative cluster. The thick line represents the linear fit averaged across subjects. The topography presents the significant negative cluster (8–13 Hz, 1.12–1.92 s). Illustrated sensors mark cluster membership. **B:** Correlation of delta ITPC and alpha power. The left panel shows the correlation of slow-delta ITPC and alpha power on foreperiod bins averaged across subjects. The right panel shows the correlation of slow-delta ITPC and alpha power on participants averaged across foreperiod bins.

between the variable onset times of stimulus events across the experiment (foreperiod durations between 0.6 and 1.8 s) and the frequency of the recruited neural oscillator. In previous studies, increased neural phase locking has been found at the stimulation frequency of rhythmically presented stimuli (Cravo et al., 2013; Henry & Obleser, 2012; Herrmann et al., 2013; Lakatos et al., 2013; Mathewson et al., 2012). In the present study, the stimulation frequency varied considerably across trials, but the instantaneous probability of stimulus occurrence always increased with the passage of time within a limited range (see Figure 1B). The present data suggest that, in particular, low frequency neural oscillations matched best to specifically the longest foreperiods occurring across an experiment (here 1.8 s, relating to  $\sim 0.6$  Hz) can reflect the formation of temporal expectations.

Interestingly, we observed a negative correlation between phase coherence and foreperiod duration in a slightly higher delta frequency range corresponding to the shortest foreperiods presented in the current study (here 0.6 Hz, relating to  $\sim 1.67$  Hz). One possible explanation for the reversal in this relationship is related to the correspondence of the period of a neural oscillation in a particular frequency band to the duration of a foreperiod. That is, whereas the period of a 0.6 Hz neural oscillation would allow for precise alignment of its excitable phase with S1 onset after a long foreperiod, a faster oscillation (with a shorter period) would allow for the precise

alignment of excitability with a syllable occurring after a short foreperiod has elapsed. Since shorter foreperiods would be associated with stronger phase locking in the higher delta band, a negative correlation would result. Moreover, high-excitability phases of slower neural oscillations (i.e., after longer foreperiods) could be expected to align more precisely than phases of faster neural oscillations (i.e., after shorter foreperiods) because equivalent shifts in absolute time translate to smaller phase differences for slower oscillations than for faster oscillations. This would suggest a cascading reliance on neural oscillations in decreasing frequency bands (for which the periods match the distribution of presented foreperiods) as a mechanism underlying the development of hazard-rate temporal expectations that increase in strength with the passage of time. However, it is important to note that the cluster in which we observed the negative correlation extended into higher frequency bands was stronger prior to S1 onset, and showed predominantly a posterior topography. It is thus likely to reflect, at least in part, a correspondence between foreperiod duration and the visual response evoked by the cue offset. We thus suggest that the significant cluster reflects a mixture of visual evoked effects and delta phase coherence effects that cannot be well separated using the current paradigm. Future research making use of different trial timing and foreperiod durations will be able to disentangle the contributions of these two neural sources to the observed negative correlation.

### Effects of Temporal Expectations on Alpha Power

Interestingly, despite the absence of a behavioral modulation by foreperiod duration, a benefit from increased temporal expectations emerged in the neural dynamics during subsequent syllable retention in memory: the stronger the instantaneous expectation for stimulus occurrence, the lower the centroparietal alpha power during retention of the first syllable. High alpha power has been related to increased cognitive load (e.g., Haegens, Osipova, Oostenveld, & Jensen, 2010; Jensen, Gelfand, Kounios, & Lisman, 2002; Klimesch, 2012; Leiberg, Lutzenberger, & Kaiser, 2006) and has further been shown to be relatively decreased under the beneficial influence of temporal cues for stimuli in noise (Wilsch et al., 2014) or with improved quality of the sensory input (Obleser et al., 2012). Hence, lowered alpha power during syllable retention after longer foreperiods is the best indicator in the present data that temporal expectations as a function of foreperiod duration not only optimize sensory processes but also reduce cognitive load.

But can we establish direct links between temporal expectations, slow neural phase concentration, and later alpha power effects? Average slow-delta phase locking across participants and the respective alpha power correlated negatively when treating foreperiod bins as the units of observation (Figure 3A). However, a partial correlation controlling for foreperiod duration showed that increased temporal expectations (from bin 1 to bin 7) were the common driver of the increase in slow-delta phase locking and the decrease in alpha power, respectively. More interestingly, individuals' average degree of slow-delta phase locking predicted their later average degree of alpha power (Figure 3B, right panel). Thus, individuals with higher slow-delta phase coherence during stimulus encoding exhibited lower alpha power during later memory retention. This is at least initial evidence that temporal expectations benefit retention in memory (Wilsch et al., 2014) by way of optimized neural phase organization around the time point of stimulus encoding.

### Topography of Slow-Delta Phase Concentration

The observed slow-delta band phase locking difference emerged most prominently at right frontotemporal sensors. This topography suggests at least two possible generators. First, the topographies in Figure 2D indicate that slow-delta ITPC has its peak at temporal sites and thus most likely emerged from sources in the superior temporal gyrus. This possibility is in line with previous studies that have reported increased delta-phase coherence predominantly in the primary sensory areas corresponding to the modality of the anticipated stimulus (Lakatos et al., 2005, 2008). The statistical effect, however, appears to be more frontally located. Thus, the same topographical distribution of statistical effects also allows for the possibility that phase-locking effects emerged at least partly from the cingulo-opercular network. This network plays a critical role in attentional control over diverse cognitive processes such as perception and decision making (Dosenbach et al., 2007; Eckert et al., 2009; Sadaghiani, Hesselmann, & Kleinschmidt, 2009). Hence, enhanced activation of these brain regions has been shown

to be favorable for stimulus processing (e.g., Vaden et al., 2013). A previous, near-threshold instantiation of the present design also yielded neural oscillatory (alpha power) modulations with a comparable topography and right anterior insula source localization (Wilsch et al., 2014).

The former interpretation supports the idea that changes in slow-delta phase coherence reflect perceptual modulation directly in sensory regions (i.e., auditory cortex). In contrast, the latter suggests that slow-delta phase coherence is an attentional signal originating from domain-general cortex. While requiring future disambiguation, both interpretations are in line with improved stimulus processing through temporal expectations, by way of neural phase realignment.

In closing, one should acknowledge the summated and indirect nature of the MEG signal. Resulting from this, the current data cannot separate changes in evoked magnetic field activity from true altered phase concentration of ongoing neural oscillations. According to Ding and Simon (2013), intertrial phase coherence is much more sensitive to stimulus-synchronized neural activity than are measures of power. In our study, neither total nor evoked power were sensitive enough to capture significant variations whereas phase coherence was. However, the similarity of patterns between phase locking and evoked power leaves open whether the underlying neural process is a change in oscillatory phase patterns or in amplitude, or in both.

Lastly, note that in the present study the explicit temporal cue whose offset in turn marked the onset of the foreperiod was a visual stimulus whereas the target was auditory. Hence, increased neural phase coherence in the delta band might be caused by a cross-modal phase reset where the attended stimuli in one sensory modality can affect processing of inputs in another modality (Busse, Roberts, Crist, Weissman, & Woldorff, 2005). Specifically, a visual stimulus signaling an upcoming auditory stimulus has been shown to reset auditory cortical oscillations to a state of high excitability (Lakatos et al., 2009; Thome et al., 2011; Thome & Debener, 2013). Despite the fact that the mentioned studies applied a much shorter stimulus onset asynchrony between a visual and an auditory target (30 to 75 ms; Thome et al., 2011) our design with much longer stimulus onset asynchronies (i.e., foreperiod durations between 0.6 and 1.8 s) might be reflecting an extended, but closely related form of cross-modal phase reset.

### Conclusions

In sum, we here have shown that temporal expectations are formed and utilized based on highly variable, probabilistic event occurrences. Furthermore, unlike more explicit, controlled expectations (like those elicited by the visual cues in the current study), these temporal expectations also impact the sensory processing of suprathreshold stimuli. Phase precision of slow neural oscillations in a slow-delta frequency range that matched the temporal scale of the experimental manipulation increases as temporal expectations become more precise. These data thus underline the utility of slow neural oscillations in understanding processes of perceptual organization and attentional control.

### References

- Barnes, R. & Jones, M. R. (2000). Expectancy, attention, and time. *Cognitive Psychology*, *41*, 254–311. doi:10.1006/cogp.2000.0738
- Busse, L., Roberts, K. C., Crist, R. E., Weissman, D. H., & Woldorff, M. G. (2005). The spread of attention across modalities and space in a multisensory object. *Proceedings of the National Academy of Sciences of the United States of America*, *102*, 18751–18756. doi:10.1073/pnas.0507704102
- Correa, A., Lupiáñez, J., & Tudela, P. (2006). The attentional mechanism of temporal orienting: Determinants and attributes. *Experimental Brain Research*, *169*, 58–68. doi:10.1007/s00221-005-0131-x

- Correa, A., & Nobre, A. C. (2008). Neural modulation by regularity and passage of time. *Journal of Neurophysiology*, *100*, 1649–1655. doi:10.1152/jn.90656.2008
- Coull, J. T., & Nobre, A. C. (1998). Where and when to pay attention: The neural systems for directing attention to spatial locations and to time intervals as revealed by both PET and fMRI. *Journal of Neuroscience*, *18*, 7426–7435. doi:0270-6474/98/187426-10\$05.00/0
- Cravo, A. M., Rohenkohl, G., Wyart, V., & Nobre, A. C. (2013). Temporal expectation enhances contrast sensitivity by phase entrainment of low-frequency oscillations in visual cortex. *Journal of Neuroscience*, *33*, 4002–4010. doi:10.1523/JNEUROSCI.4675-12.2013
- David, O., Kilner, J., & Friston, K. (2006). Mechanisms of evoked and induced responses in MEG/EEG. *NeuroImage*, *31*, 1580–1591. doi:10.1016/j.neuroimage.2006.02.034
- Ding, N., & Simon, J. Z. (2013). Power and phase properties of oscillatory neural responses in the presence of background activity. *Journal of Computational Neuroscience*, *34*, 337–343. doi:10.1007/s10827-012-0424-6.Power
- Doherty, J. R., Rao, A., Mesulam, M. M., & Nobre, A. C. (2005). Synergistic effect of combined temporal and spatial expectations on visual attention. *Journal of Neuroscience*, *25*, 8259–8266. doi:10.1523/JNEUROSCI.1821-05.2005
- Dosenbach, N. U. F., Fair, D. A., Miezin, F. M., Cohen, A. L., Wenger, K. K., Dosenbach, R. A. T., . . . Petersen, S. E. (2007). Distinct brain networks for adaptive and stable task control in humans. *Proceedings of the National Academy of Sciences of the United States of America*, *104*, 11073–11078. doi:10.1073/pnas.0704320104
- Eckert, M. A., Menon, V., Walczak, A., Ahlstrom, J. B., Denslow, S., Horwitz, A., & Dubno, J. R. (2009). At the heart of the ventral attention system: The right anterior insula. *Human Brain Mapping*, *30*, 2530–2541. doi:10.1002/hbm.20688
- Haegens, S., Osipova, D., Oostenveld, R., & Jensen, O. (2010). Somatosensory working memory performance in humans depends on both engagement and disengagement of regions in a distributed network. *Human Brain Mapping*, *31*, 26–35. doi:10.1002/hbm.20842
- Hämäläinen, M., Hari, R., Ilmoniemi, R. J., Knuutila, J., & Lounasmaa, O. (1993). Magnetoencephalography—Theory, instrumentation, and applications to noninvasive studies of the working human brain. *Reviews of Modern Physics*, *65*, 413–497. doi:10.1103/RevModPhys.65.413
- Henry, M. J., & Herrmann, B. (2014). Low-frequency neural oscillations support dynamic attending in temporal context. *Timing & Time Perception*, *2*, 62–86. doi:10.1163/22134468-00002011
- Henry, M. J., & Obleser, J. (2012). Frequency modulation entrains slow neural oscillations and optimizes human listening behavior. *Proceedings of the National Academy of Sciences of the United States of America*, *109*, 20095–20100. doi:10.1073/pnas.1213390109
- Herrmann, B., Henry, M. J., Grigutsch, M., & Obleser, J. (2013). Oscillatory phase dynamics in neural entrainment underpin illusory percepts of time. *Journal of Neuroscience*, *33*, 15799–15809. doi:10.1523/JNEUROSCI.1434-13.2013
- Janssen, P., & Shadlen, M. (2005). A representation of the hazard rate of elapsed time in macaque area LIP. *Nature Neuroscience*, *8*, 234–241.
- Jensen, O., Gelfand, J., Kounios, J., & Lisman, J. E. (2002). Oscillations in the alpha band (9–12 Hz) increase with memory load during retention in a short-term memory task. *Cerebral Cortex*, *12*, 877–882. doi:10.1038/nn1386
- Jones, M. R., Moynihan, H., MacKenzie, N., & Puente, J. (2002). Temporal aspects of stimulus-driven attending in dynamic arrays. *Psychological Science*, *13*, 313–319. doi:10.1111/1467-9280.00458
- Klimesch, W. (2012). Alpha-band oscillations, attention, and controlled access to stored information. *Trends in Cognitive Sciences*, *16*, 606–617. doi:10.1016/j.tics.2012.10.007
- Lachaux, J. P., Rodriguez, E., Martinerie, J., & Varela, F. J. (1999). Measuring phase synchrony in brain signals. *Human Brain Mapping*, *8*, 194–208.
- Lakatos, P., Karmos, G., Mehta, A. D., Ulbert, I., & Schroeder, C. E. (2008). Entrainment of neuronal oscillations as a mechanism of attentional selection. *Science*, *320*, 110–113. doi:10.1126/science.1154735
- Lakatos, P., O’Connell, M. N., Barczak, A., Mills, A., Javitt, D. C., & Schroeder, C. E. (2009). The leading sense: Supramodal control of neurophysiological context by attention. *Neuron*, *64*, 419–430. doi:10.1016/j.neuron.2009.10.014
- Lakatos, P., Schroeder, C. E., Leitman, D. I., & Javitt, D. C. (2013). Predictive suppression of cortical excitability and its deficit in schizophrenia. *Journal of Neuroscience*, *33*, 11692–11702. doi:10.1523/JNEUROSCI.0010-13.2013
- Lakatos, P., Shah, A. S., Knuth, K. H., Ulbert, I., Karmos, G., & Schroeder, C. E. (2005). An oscillatory hierarchy controlling neuronal excitability and stimulus processing in the auditory cortex. *Journal of Neurophysiology*, *94*, 1904–1911. doi:10.1152/jn.00263.2005
- Lange, K., & Schnuerch, R. (2014). Challenging perceptual tasks require more attention: The influence of task difficulty on the N1 effect of temporal orienting. *Brain and Cognition*, *84*, 153–163. doi:10.1016/j.bandc.2013.12.001
- Large, E. W., & Jones, M. R. (1999). The dynamics of attending: How people track time-varying events. *Psychological Review*, *106*, 119–159. doi:10.1037//0033-295X.106.1.119
- Lawrance, E. L. A., Harper, N. S., Cooke, J. E., & Schnupp, J. W. H. (2014). Sources in the superior temporal gyrus or the auditory cortex. *Journal of the Acoustical Society of America*, *135*, EL357–EL363. doi:10.1121/1.4879667
- Leiberg, S., Lutzenberger, W., & Kaiser, J. (2006). Effects of memory load on cortical oscillatory activity during auditory pattern working memory. *Brain Research*, *1120*, 131–140. doi:10.1016/j.brainres.2006.08.066
- Maris, E., & Oostenveld, R. (2007). Nonparametric statistical testing of EEG- and MEG-data. *Journal of Neuroscience Methods*, *164*, 177–190. doi:10.1016/j.jneumeth.2007.03.024
- Mathewson, K. E., Prudhomme, C., Fabiani, M., Beck, D. M., Lleras, A., & Gratton, G. (2012). Making waves in the stream of consciousness: Entraining oscillations in EEG alpha and fluctuations in visual awareness with rhythmic visual stimulation. *Journal of Cognitive Neuroscience*, *24*, 2321–2333. doi:10.1162/jocn\_a\_00288
- Nobre, A. C. (2001). Orienting attention to instants in time. *Neuropsychologia*, *39*, 1317–1328. doi:10.1016/S0028-3932(01)00120-8
- Nobre, A. C., Correa, A., & Coull, J. T. (2007). The hazards of time. *Current Opinion in Neurobiology*, *17*, 465–470. doi:10.1016/j.conb.2007.07.006
- Obleser, J., Wöstmann, M., Hellbernd, N., Wilsch, A., & Maess, B. (2012). Adverse listening conditions and memory load drive a common alpha oscillatory network. *Journal of Neuroscience*, *32*, 12376–12383. doi:10.1523/JNEUROSCI.4908-11.2012
- Oostenveld, R., Fries, P., Maris, E., & Schoffelen J.-M. 2011. FieldTrip: Open source software for advanced analysis of MEG, EEG, and invasive electrophysiological data. *Computational Intelligence and Neuroscience*, *2011*, 156869. doi:10.1155/2011/156869
- Penttonen, M. (2003). Natural logarithmic relationship between brain oscillators. *Thalamus & Related Systems*, *2*, 145–152. doi:10.1016/S1472-9288(03)00007-4
- Rohenkohl, G., Coull, J. T., & Nobre, A. C. (2011). Behavioural dissociation between exogenous and endogenous temporal orienting of attention. *PLoS ONE*, *6*, e14620. doi:10.1371/journal.pone.0014620
- Rohenkohl, G., Cravo, A. M., Wyart, V., & Nobre, A. C. (2012). Temporal expectation improves the quality of sensory information. *Journal of Neuroscience*, *32*, 8424–8428. doi:10.1523/JNEUROSCI.0804-12.2012
- Rosenthal, R. (1994). Parametric measures of effect size. In H. Cooper & L. V. Hedges (Eds.), *Handbook of research synthesis* (pp. 231–244). New York, NY: Russell Sage Foundation.
- Sadaghiani, S., Hesselmann, G., & Kleinschmidt, A. (2009). Distributed and antagonistic contributions of ongoing activity fluctuations to auditory stimulus detection. *Journal of Neuroscience*, *29*, 13410–13417. doi:10.1523/JNEUROSCI.2592-09.2009
- Sanabria, D., & Correa, A. (2013). Electrophysiological evidence of temporal preparation driven by rhythms in audition. *Biological Psychology*, *92*: 98–105. doi:10.1016/j.biopsycho.2012.11.012
- Schroeder, C. E., & Lakatos, P. (2009). Low-frequency neuronal oscillations as instruments of sensory selection. *Trends in Neurosciences*, *32*, 9–18. doi:10.1016/j.tins.2008.09.012
- Stefanics, G., Hangya, B., Hernádi, I., Winkler, I., Lakatos, P., & Ulbert, I. (2010). Phase entrainment of human delta oscillations can mediate the effects of expectation on reaction speed. *Journal of Neuroscience*, *30*, 13578–13585. doi:10.1523/JNEUROSCI.0703-10.2010
- Steriade, M., Nunez, A., & Amzica, F. (1993). A novel slow (<1 Hz) oscillation of neocortical neurons in vivo: Depolarizing and hyperpolarizing components. *Journal of Neuroscience*, *13*, 3252–3265.

- Taulu, S., Kajola, M., & Simola, J. (2004). Suppression of interference and artifacts by the signal space separation method. *Brain Topography*, *16*, 269–275.
- Thorne, J. D., De Vos, M., Viola, F. C., & Debener, S. (2011). Cross-modal phase reset predicts auditory task performance in humans. *Journal of Neuroscience*, *31*, 3853–3861. doi:10.1523/JNEUROSCI.6176-10.2011
- Thorne, J. D., & Debener, S. (2013). Look now and hear what's coming: On the functional role of cross-modal phase reset. *Hearing Research*, *307*, 144–152. doi:10.1016/j.heares.2013.07.002
- van Dijk, H., Nieuwenhuis, I. L. C., & Jensen, O. (2010). Left temporal alpha band activity increases during working memory retention of pitches. *European Journal of Neuroscience*, *31*, 1701–1707. doi:10.1111/j.1460-9568.2010.07227.x
- Vaden, K. I., Kuchinsky, S. E., Cute, S. L., Ahlstrom, J. B., Dubno, J. R., & Eckert, M. A. (2013). The cingulo-opercular network provides word-recognition benefit. *Journal of Neuroscience*, *33*, 18979–18986. doi:10.1523/JNEUROSCI.1417-13.2013
- Wilsch, A., Henry, M. J., Herrmann, B., Maess, B., & Obleser, J. (2014). Alpha oscillatory dynamics index temporal expectation benefits in working memory. *Cerebral Cortex*, 1–9. Advance online publication. doi:10.1093/cercor/bhu004

(RECEIVED July 28, 2014; ACCEPTED December 10, 2014)